Zinc Excess Induces a Hypoxia-Like Response by Inhibiting Cysteine Oxidases in Poplar Roots[1][OPEN]

Laura Dalle Carbonare,[a] Mark D. White,[b] Vinay Shukla,[a] Alessandra Francini,[a] Pierdomenico Perata,[a] Emily Flashman,[b] Luca Sebastiani,[a] and Francesco Licausi[a,c,2,3]

[a]PlantLab, Institute of Life Sciences, Scuola Superiore Sant'Anna, 56127 Pisa, Italy
[b]Department of Chemistry, University of Oxford, Oxford OX1 3TA, United Kingdom
[c]Biology Department, University of Pisa, 56126 Pisa, Italy

ORCID IDs: 0000-0001-9444-0610 (P.P.); 0000-0003-4769-441X (F.L.).

Poplar (*Populus* spp.) is a tree species considered for the remediation of soil contaminated by metals, including zinc (Zn). To improve poplar's capacity for Zn assimilation and compartmentalization, it is necessary to understand the physiological and biochemical mechanisms that enable these features as well as their regulation at the molecular level. We observed that the molecular response of poplar roots to Zn excess overlapped with that activated by hypoxia. Therefore, we tested the effect of Zn excess on hypoxia-sensing components and investigated the consequence of root hypoxia on poplar fitness and Zn accumulation capacity. Our results suggest that high intracellular Zn concentrations mimic iron deficiency and inhibit the activity of the oxygen sensors Plant Cysteine Oxidases, leading to the stabilization and activation of ERF-VII transcription factors, which are key regulators of the molecular response to hypoxia. Remarkably, excess Zn and waterlogging similarly decreased poplar growth and development. Simultaneous excess Zn and waterlogging did not exacerbate these parameters, although Zn uptake was limited. This study unveils the contribution of the oxygen-sensing machinery to the Zn excess response in poplar, which may be exploited to improve Zn tolerance and increase Zn accumulation capacity in plants.

Zinc (Zn) is the second most abundant transition metal, after iron, in living organisms (Broadley et al., 2007), where it is considered an essential micronutrient required to complete the life cycle. In particular, Zn is the only metal represented in all six enzyme classes (oxidoreductases, transferases, hydrolases, lyases, isomerases, and ligases; Coleman, 1998; Broadley et al., 2007; Bouain et al., 2014) and plays a structural, catalytic, or cocatalytic role in more than 300 proteins (Broadley et al., 2007; Ricachenevsky et al., 2015). Plants acquire Zn from the soil as free Zn^{2+}, whose availability depends mainly on the soil composition and pH (Bouain et al., 2014). Furthermore, some plant species are able to release organic metal chelators in the rhizosphere in order to take the metal up more efficiently (Ricachenevsky et al., 2015). From the roots, Zn is distributed to stems and leaves through the xylematic flux (Sinclair and Krämer, 2012). Although Zn levels in eukaryotic cells stand in the range of 100 μM, the concentration of free Zn^{2+} in the cytosol is usually maintained below the nanomolar range, thus preventing interference with metal-associated proteins (Sinclair and Krämer, 2012). This tight control of Zn^{2+} concentration is achieved through Zn high-affinity binding to phytochelatins, metallothioneins, and organic acids in the cytosol and through compartmentalization of this metal into cell vacuoles (Broadley et al., 2007; Ricachenevsky et al., 2015; Sharma et al., 2016).

Zn concentrations above 300 $\mu g\ g^{-1}$ induce visible toxicity symptoms, including root and shoot growth impairment, leaf chlorosis, and interference with P, Mg, and Mn uptake (Broadley et al., 2007; Yadav, 2010). Zn accumulates in soils and water as a consequence of anthropogenic activities such as mining, smelting, and fertilization with sewage sludge, thereby leading to Zn contamination (Broadley et al., 2007; Yadav, 2010; Sinclair and Krämer, 2012; Shi et al., 2015). Currently, phytoremediation is a cost-effective technology to clean up Zn-polluted soils, exploiting the natural capacity of some plants to absorb and transport heavy metals from the soil to the vegetative tissues (Pilon-Smits, 2005). Among plants, *Populus* spp. (poplar) are among of the most suitable for metal phytoremediation, due to their rapid growth rate, large aboveground biomass, deep

[1]This work was supported by the Ph.D. Program in Agrobiosciences of the Scuola Superiore Sant'Anna (to L.D.C. and V.S.) and by the Biotechnology and Biological Sciences Research Council (New Investigator grant BB/M024458/1 to M.D.W. and E.F.).

[2]Author for contact: francesco.licausi@unipi.it.
[3]Senior author.

The author responsible for distribution of materials integral to the findings presented in this article in accordance with the policy described in the Instructions for Authors (www.plantphysiol.org) is: Francesco Licausi (francesco.licausi@unipi.it).

L.D.C., A.F., L.S., and F.L. defined the aims of the project and planned the activities; L.D.C. performed all experiments and analyzed their results; M.D.W. produced recombinant PCO proteins and, together with E.F., supervised the biochemical assays; V.S. carried out confocal microscopy observations; L.D.C. and F.L. wrote the article; P.P. and L.S. critically assessed and edited the article.

[OPEN]Articles can be viewed without a subscription.

www.plantphysiol.org/cgi/doi/10.1104/pp.18.01458

root penetration, and, depending on the species, the ability to accumulate a broad range of metal concentrations (Shi et al., 2015). Depending on the cultivar, poplar trees are either tolerant or sensitive to the excess of heavy metals, which ultimately influences their accumulation capacity (Pajevi et al., 2016). In this work, we selected two poplar species: *Populus alba* 'Villafranca' clone, which is comparatively Zn tolerant, and the hybrid poplar *Populus* × *canadensis* (*Populus deltoides* × *Populus nigra*) 'I-214' clone, which displays Zn sensitivity (Romeo et al., 2014). The phenotypic response of both varieties to Zn excess has been well characterized previously (Di Baccio et al., 2003, 2005, 2009; Romeo et al., 2014, 2017).

Poplar trees thrive in several habitats from forests to riparian ecosystems (Müller et al., 2013), the latter of which are regularly flooded, and therefore, this tree species is considered as waterlogging and flooding tolerant (Kreuzwieser et al., 2002). Flooding is typically considered as a stress factor due to the reduction of gas diffusion in water as compared with that in air. Indeed, a drop in oxygen levels occurs in waterlogged terrains, and it is exacerbated by competitive microorganism respiration (Sasidharan et al., 2018). Low oxygen levels in the soil affect the development and performance of roots, since the establishment of hypoxic conditions impairs mitochondrial respiration, oxidation, and oxygenation processes (Kreuzwieser et al., 2002), and consequently the fitness of the whole plant.

The response of plants to low oxygen availability has been extensively characterized and proposed to be regulated by the concerted action of group VII Ethylene Response Factors (ERF-VIIs) and Plant Cysteine Oxidase (PCO) enzymes (Banti et al., 2013; van Dongen and Licausi, 2015). Briefly, under normoxia, constitutively expressed ERF-VIIs are constantly degraded by virtue of a conserved N-terminal sequence (MCGGAI) that acts as a degradation-stimulating domain, namely N-degron (Gibbs et al., 2011; Licausi et al., 2011; Varshavsky, 2019). In the presence of oxygen and nitric oxide, oxidation of the exposed Cys in the ERF-VII degron (Gibbs et al., 2014; Weits et al., 2014) generates a potential substrate for arginylation by arginyl transferases (ATE) and subsequent polyubiquitination by the E3 ubiquitin-ligase PROTEOLYSIS6 (PRT6; Graciet and Wellmer, 2010). As a final result of these post-transcriptional modifications, ERF-VIIs are targeted to the 26S proteasome complex to be degraded. Cys oxidation is catalyzed by oxygen-dependent PCOs so that when oxygen availability decreases, PCO activity is impaired and therefore the ERF-VIIs are stabilized, leading to their accumulation in the nucleus, where they regulate specific molecular responses to anaerobiosis (Kosmacz et al., 2015; Gasch et al., 2016). In Arabidopsis (*Arabidopsis thaliana*), two ERF-VII transcription factors, namely RAP2.2 and RAP2.12, have been shown to be required to activate this molecular adaptation by binding to a conserved AAAACCA[G/C][G/C]GC DNA element defined as the Hypoxia Responsive Promoter Element (HRPE; Bui et al., 2015; Gasch et al., 2016).

Interestingly, floodplain wetlands, which are common habitats for poplars, are more often contaminated by heavy metals than dry soils, due to increased metal availability from the soil (Abdullah, 2015). As a consequence of ore extraction and processing in particular, heavy metal residuals are often discharged into river waters, and subsequent flood events can promote remobilization of the metals and dispersal into the surrounding areas (Ciszewski and Grygar, 2016).

Since flooding and metal contamination are often joint environmental cues, the possibility to apply a plant-based remediation approach must rely on species that can adapt to both conditions. In this work, we investigated the overlap of the molecular response of poplar roots to Zn excess and low-oxygen conditions. We elucidated the potential of this genus to cope with a combination of the two stresses from a molecular and physiological perspective, in order to evaluate its fitness and its performance regarding Zn accumulation.

RESULTS

Zn Excess Induces Low-Oxygen Gene Responses in Poplar Roots

The molecular response underlying the physiological sensitivity of *P. canadensis* ('I-214' clone) to excess Zn has been characterized by Ariani et al. (2015) through an RNA sequencing analysis in roots. By looking at this data set, we were struck by the apparently high occurrence of genes previously associated with the anaerobic response in different plant species. Inspired by this, we carried out a thorough comparison of the transcriptional response to Zn stress with that of gray poplar (*Populus* × *canescens*) roots subjected to prolonged waterlogging (Kreuzwieser et al., 2009), a condition involving insufficient oxygen provision. Thirty-nine percent of the 77 genes regulated by Zn excess were also differentially expressed in the waterlogging data set. The expression pattern of these 30 Zn- and hypoxia-responsive genes in poplar seems to follow the same regulation as their Arabidopsis orthologs under hypoxic conditions (Licausi et al., 2010, 2011; Fig. 1A; Supplemental Table S1). In particular, the highest similarity in the transcriptional regulation pattern between poplar and Arabidopsis was observed among the up-regulated genes.

The overlap observed between the two transcriptional adaptations could still be observed by looking at a broader data set of poplar Zn-responsive genes obtained by Ariani et al. (2015) and applying less stringent parameters (χ^2 test, not corrected P value). However, in this case, only 4% of the total Zn-related genes (20 out of 502) responded also to low-oxygen conditions (Fig. 1B; Supplemental Table S2).

Swapping perspective, we observed that 17 (35%) genes of the 49 that constitute the core molecular

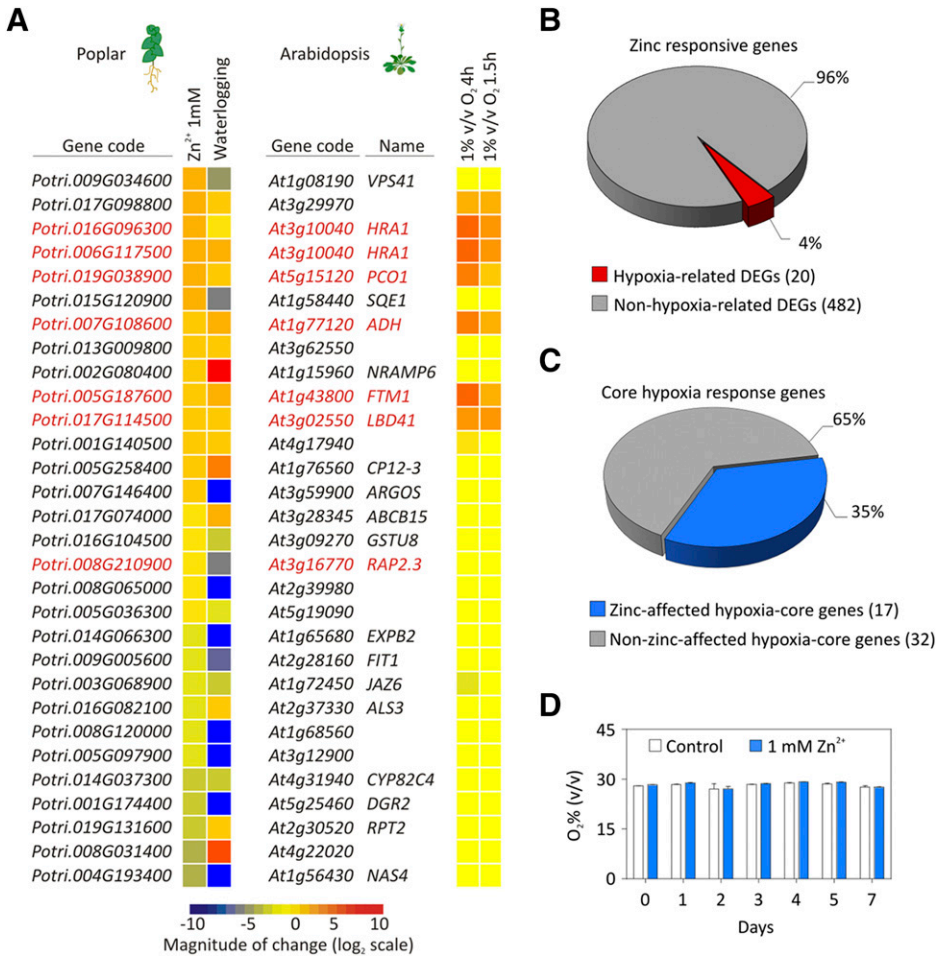

Figure 1. Molecular response to Zn overlaps with low-oxygen transcription regulation in poplar. A, Heat map showing common differentially expressed genes (DEGs) in poplar roots under 1 mM $Zn(NO_3)_2$ (Ariani et al., 2015; data set defined by χ^2 test, Bonferroni corrected $P < 0.1$) and those genes altered after 168 h of soil hypoxia (Kreuzwieser et al., 2009) compared with their Arabidopsis orthologs after 1.5 or 4 h of hypoxia (1% [v/v] oxygen/N_2; Licausi et al., 2010, 2011). Red indicates hypoxia core genes. B, Percentage of hypoxia-affected genes identified among the total Zn DEGs (Ariani et al., 2015; data set defined by χ^2 test, not corrected P value). C, Percentage of Zn-regulated genes in poplar that are also part of the core hypoxia-response genes. D, Oxygen concentration (% v/v) measured in the hydroponic solution under control and 1 mM $ZnSO_4$ conditions for 7 d. Data are presented as means ± SD ($n = 150$).

response identified by Mustroph et al. (2009) were regulated by Zn excess in poplar (Fig. 1C; Supplemental Table S3).

Considered together, these observations inspired the hypothesis that Zn excess, in addition to the activation of mechanisms dedicated to metal homeostasis and reactive oxygen species scavenging (Yadav, 2010), either contributes to the reduction of oxygen availability in poplar tissues or interferes with cell signaling to elicit hypoxia-like responses at the transcript level. To address this question, we compared the oxygen concentration in the hydroponic solution where poplar plants were subjected to Zn treatment or to control conditions (Fig. 1D). The molecular oxygen dissolved in the two solutions was not significantly different, suggesting that Zn treatment itself did not increase oxygen consumption in poplar roots.

To test whether the activation of anaerobic genes under Zn stress is part of the stress symptoms manifested by these plants or is rather activated to withstand high concentrations of this metal, we compared the gene response to Zn excess in two poplar clones characterized by different tolerance extent to this stress: the *P. canadensis* 'I-214' used by Ariani et al. (2015) and *P. alba* 'Villafranca', a poplar clone characterized as Zn tolerant (Romeo et al., 2014). After 21 d of Zn treatment (1 mM $ZnSO_4$), we observed the induction of three hypoxia marker genes, namely *Alcohol Dehydrogenase* (*Pop_ADH*), *PCO* (*Pop_PCO*), and *Hypoxia Responsive Attenuator1* (*Pop_HRA1*), in the roots of both clones (Fig. 2; Supplemental Fig. 1). Moreover, the induction of the Zn-stress marker gene *ZRT, IRT-like Protein2* (*Pop_ZIP2*) confirmed the effectiveness of the treatment (Fig. 2). Since the induction of anaerobic genes did not show a clear difference between the tolerant and intolerant clones, we favored the hypothesis of poplar activating hypoxic genes as a generic response to Zn excess.

The ERF-VII Pop_ERFB2-1 Can Activate Hypoxia-Responsive Genes in Poplar

Since the molecular response to low oxygen levels in Arabidopsis has been shown to mainly rely on the ERF-VII transcription factors RAP2.2 and RAP2.12 (Bui et al., 2015; Gasch et al., 2016), we further evaluated whether similar transcriptional regulators are responsible for the observed molecular response to hypoxia under Zn stress in poplar. A systematic comparison of

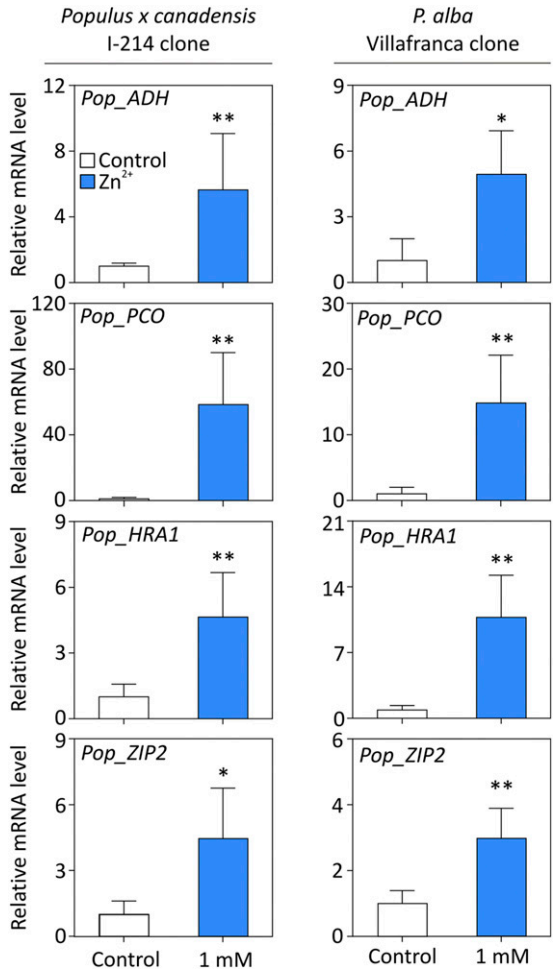

Figure 2. Zn excess promotes the molecular response to low oxygen in poplar. Induction of hypoxia (*Pop_ADH*, *Pop_PCO*, and *Pop_HRA1*) and Zn (*Pop_ZIP2*) marker genes is shown in a Zn-sensitive (*P. canadensis* 'I-214' clone) and a Zn-tolerant (*P. alba* 'Villafranca' clone) poplar species following 1 mM $ZnSO_4$ treatment for 21 d. Data are presented as means ± SD ($n = 5$); two-tailed Student's *t* test: *, $P < 0.05$ and **, $P < 0.01$.

the ERF-VIIs from Arabidopsis (Licausi et al., 2010) and *Populus trichocarpa* (Zhuang et al., 2008) in terms of amino acid sequence occurrence and position of conserved motifs (CMVII) identified by Nakano et al. (2006) allowed us to identify the relatedness between different group members (Fig. 3A). PtERFB2-1 was selected as the closest ortholog of AtRAP2.2-12, due to its high sequence similarity to the Arabidopsis transcription factors accompanied by the occurrence of eight out of nine CMVIIs (Supplemental Fig. S2; Supplemental File S1). Furthermore, we assessed the transcriptional regulation of *ERF-VII* in poplar roots under anoxic conditions and observed that *Pop_ERFB2-1/Pop_ERFB2/Pop_ERFB3/Pop_ERFB4* and *Pop_ERFB2-5/Pop_ERFB6* followed the same expression pattern as *AtRAP2.2-12-3* and *HRE1-2*, respectively (Licausi et al., 2010; Fig 3B; Supplemental Table S4).

To verify whether Pop_ERFB2-1 can actually regulate hypoxia-responsive genes in poplar, we assessed its ability to regulate a synthetic promoter bearing a five-time-repeated HRPE (5x*HRPE*; Gasch et al., 2016), which was also identified in the genomic region upstream of the poplar anaerobic genes assessed before (Supplemental Fig. S3). To this end, we transfected poplar mesophyll protoplasts with a *35S:GFP:Pop_ERFB2-1* cassette and a reporter plasmid carrying the 5x*HRPE* synthetic promoter fused to the firefly (*Photinus pyralis*) luciferase (*PpFluc*) gene (Fig. 3C), whereby luminescence was measured as a readout of promoter activation. The PpFluc activity was normalized over that of sea pansy (*Renilla reniformis*) luciferase (*35S:RrLuc*) encoded by the same reporter vector. GFP:Pop_ERFB2-1 was indeed able to strongly activate the 5x*HRPE* promoter in poplar protoplasts (Fig. 3D). Remarkably, the relative luciferase activity was significantly reduced when a stabilized version of Arabidopsis *RAP2.12*, lacking the first 13 amino acids, was cotransfected with the same synthetic promoter in poplar protoplasts (Fig. 3E). On the other hand, both stabilized forms of Pop_ERFB2-1 and RAP2.12 were seen to induce HRPE in Arabidopsis protoplasts (Fig. 3F). Thus, we concluded that Pop_ERFB2-1 is likely accountable for the induction of anaerobic genes in poplar, albeit the transactivation capacity of ERF-VII from different species relies on alternative protein partnership and regulation.

We also attempted transgenic complementation of an Arabidopsis pentuple T-DNA insertion mutant almost entirely devoid of ERF-VII activity (Abbas et al., 2015; Giuntoli et al., 2017), with consequent inhibition of the transcriptional response to low-oxygen conditions. Although the expression level of the *Pop_ERFB2-1* was confirmed in four independent transgenic lines by reverse transcription quantitative PCR (RT-qPCR), hypoxic gene expression induction after 6 h of hypoxia (1% [v/v] oxygen) was not restored (Fig. 3G). Therefore, the above results supported our hypothesis that there is different regulation imposed onto ERF-VIIs and their partners in poplar and Arabidopsis.

Pop_ERFB2-1 Stability Is Enhanced by Zn in Protoplasts

Bearing in mind that Zn excess in poplar alters the expression of hypoxia-responsive genes, which are likely under the control of Pop_ERFB2-1, we further investigated whether Zn promoted the anaerobic response through Pop_ERFB2-1. First, we measured *Pop_ERFB2-1* expression in poplar roots subjected to Zn stress and observed that its transcriptional level did not change over the course of the stress treatment (Supplemental Fig. S4).

Similar to other ERF-VII proteins characterized by a conserved N-terminal consensus, the stability of Pop_ERFB2-1 protein is expected to be controlled by the N-degron pathway. To test this assumption, we fused the entire coding sequence (CDS) of *Pop_ERFB2-1* to

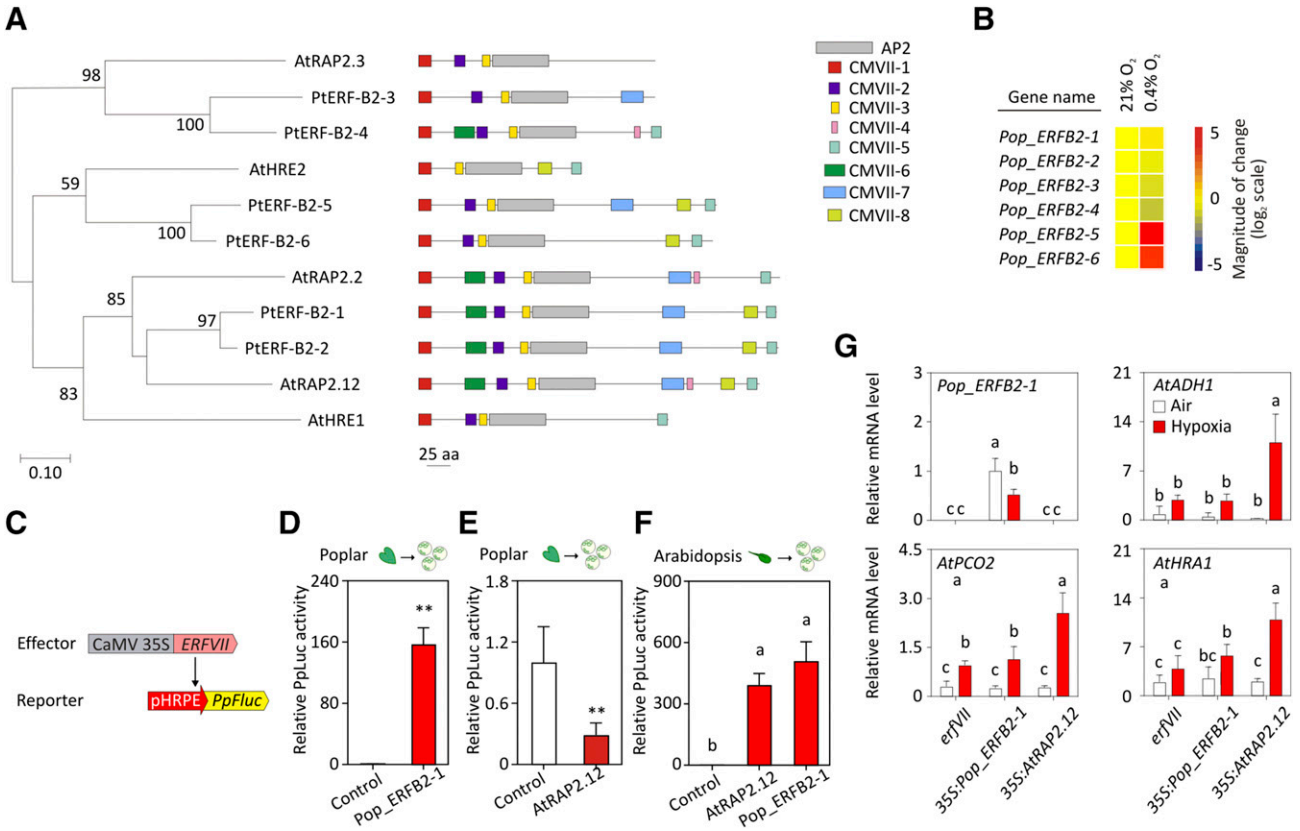

Figure 3. Characterization of the poplar ERF-VII protein, Pop_ERFB2-1. A, Phylogenetic relationship between Arabidopsis ERF-VIIs and their closest poplar orthologs (Zhuang et al., 2008), generated from a multialignment processed via the maximum-likelihood algorithm. The ERF-VII common motifs (CMVIIs) are shown on the right of each sequence. B, Heat map showing the relative expression of *Pop_ERFB2s* under normoxic (21% [v/v] oxygen) and anoxic (0% [v/v] oxygen, 4 h) conditions in poplar roots. C, Schematic representation of the experiment conducted to collect the data shown in D to F. D, Effect of Δ13RAP2.12 on the synthetic hypoxia-responsive promoter fused to the firefly luciferase (*pHRPE:PpLuc*) in poplar protoplasts. Data are presented as means ± SD ($n = 4$); **, $P < 0.01$, as calculated by two-tailed Student's *t* test. E, Effect of GFP-Pop_ERFB2-1 on *pHRPE:PpLuc* luciferase in poplar protoplasts. Data are presented as means ± SD ($n = 4$); **, $P < 0.01$, as calculated by two-tailed Student's *t* test. F, Effect of Δ13RAP2.12 and GFP-Pop_ERFB2-1 on *pHRPE:PpLuc* luciferase in Arabidopsis protoplasts. Data are presented as means ± SD ($n = 4$); different letters indicate statistically significant difference ($P < 0.01$), as calculated by two-tailed Student's *t* test. G, Complementation of the Arabidopsis pentuple *erf-VII* mutant by the constitutive expression of *Pop_ERFB2-1* and *AtRAP2.12*. Expression levels of *Pop_ERFB2-1*, *AtADH1*, *AtPCO2*, and *AtHRA1* are shown under aerobic (white bars) and 6 h of 1% (v/v) oxygen (red bars) conditions in the *erf-VII* background and in *Pop_ERB2-1*- or *AtRAP2.12*-expressing plants. Data are presented as means + SD ($n = 4$), where values for *erf-VII* complemented lines correspond to the means of four independent lines. Different letters indicate statistically different averages as assessed by two-way ANOVA followed by the Holm-Sidak posthoc test ($P < 0.05$).

PpLuc to generate a posttranscriptional reporter and transfected a vector bearing this construct into Arabidopsis protoplasts of the wild type and of mutants lacking components of the N-degron pathway (*ate1 ate2* and *prt6*). Here, higher relative luciferase activity was measured in mutant protoplasts as compared with that in wild-type protoplasts, suggesting increased stability of the chimeric protein in the former cells (Fig. 4A). Consequently, we investigated whether its constitutive proteolysis is inhibited by exposure to Zn excess using a transient transformation system based on poplar mesophyll protoplasts. First, we verified whether ERF-VII activity is enhanced by Zn treatment also in this system by looking at the activation of the synthetic reporter *pHRPE:PpLuc* in the presence of 200 μM $ZnSO_4$. Sixteen hours of Zn supplementation was necessary to observe an increase in ERF-VII activity, whereas a short exposure to high concentrations of this metal did not affect its expression (Fig. 4B). Next, we used the same *Pop_ERFB2-1:PpLuc* cassette to transfect poplar protoplasts supplemented with a range of Zn concentrations spanning from 0 to 800 μM for 16 h (Fig. 4C). We observed a significant increase in the luciferase activity for Zn concentrations above 100 μM, showing that Pop_ERFB2-1 protein stability was enhanced under Zn excess in protoplasts. Comparably, a chimeric reporter, consisting of the first 28 amino acids of AtRAP2.12 fused to the N terminus of PpLuc, was stabilized in

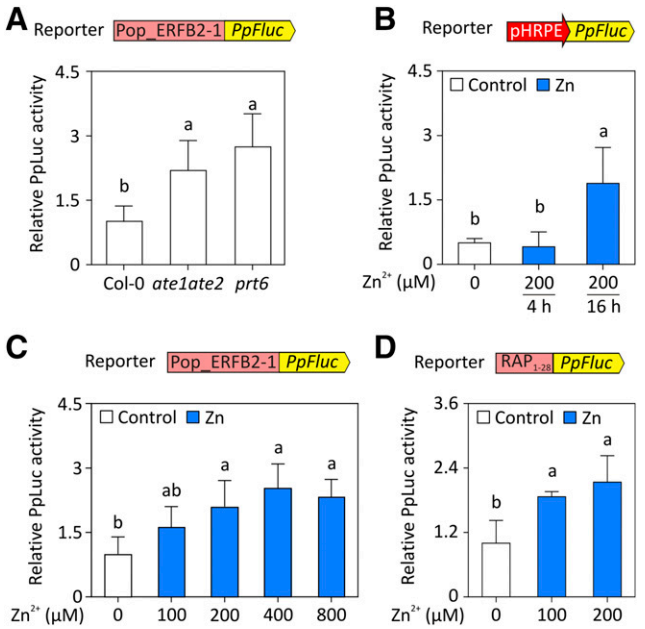

Figure 4. Zn effect on Pop_ERFB2-1 stability and activity. A, Relative luciferase activity of PpLuc fused to Pop_ERFB2-1 in protoplasts of wild-type Columbia-0 (Col-0) and *ate1 ate2* and *prt6* Arabidopsis mutants. B, Effect of 200 μM Zn on PpLuc expression driven by the *pHRPE* promoter after 4 or 16 h of treatment in poplar protoplasts. C, Effect of an overnight treatment with a range of Zn concentrations (from 0 to 800 μM) on Pop_ERFB2-1-PpLuc activity in poplar protoplasts. D, Relative luciferase activity of PpLuc fused to the first 28 amino acids of Arabidopsis RAP2.12 after an overnight treatment with 100 or 200 μM Zn in Arabidopsis protoplasts. Data are shown as means ± SD (n = 5). Different letters indicate significant differences ($P < 0.05$, one-way ANOVA followed by the Holm-Sidak posthoc test).

Arabidopsis protoplasts treated with 100 or 200 μM Zn for 16 h (Fig. 4D). Thus, we concluded that the up-regulation of hypoxia-responsive genes following Zn stress in poplar was explained by the increased stability, and thereby activity, of Pop_ERFB2-1 and possibly other poplar ERF-VIIs.

Zn Inhibits PCO Activity in Vitro

In view of the capacity of Zn excess to cause Pop_ERFB2-1 stabilization under aerobic conditions, we assumed that one of the steps of the N-degron pathway should be hindered by Zn itself. Among the enzymes involved in addressing ERF-VII toward proteolysis, PCOs are dioxygenases that catalyze the oxidation of the conserved Cys at the N terminus of the ERF-VIIs (White et al., 2017). Since PCO activity seems to rely on the presence of Fe(II) in the active site (White et al., 2017, 2018), we hypothesized that the bivalent cation Zn^{2+} could compete with Fe(II) for the active site of the enzyme and impair its activity. We therefore used the AtPCO1 amino acid sequence as a query to identify putative PCO orthologs encoded in the *P. trichocarpa* genome and found eight that clustered together with their Arabidopsis counterparts to generate two main clades (Fig. 5A; Supplemental File S2). We chose one poplar PCO for each cluster, specifically Potri.017G079400 and Potri.012G057400 as closest orthologs of AtPCO1-2 and AtPCO3-4-5, respectively, and we measured their Cys oxidation activity on a 14-amino acid peptide, corresponding to the N terminus of Pop_ERFB2-1. First, we tested in vitro whether the activity of the two poplar PCOs could be affected by an excess of three different cations (Zn^{2+}, Ca^{2+}, and Cd^{2+}) dissolved in the enzymatic solution and free to access

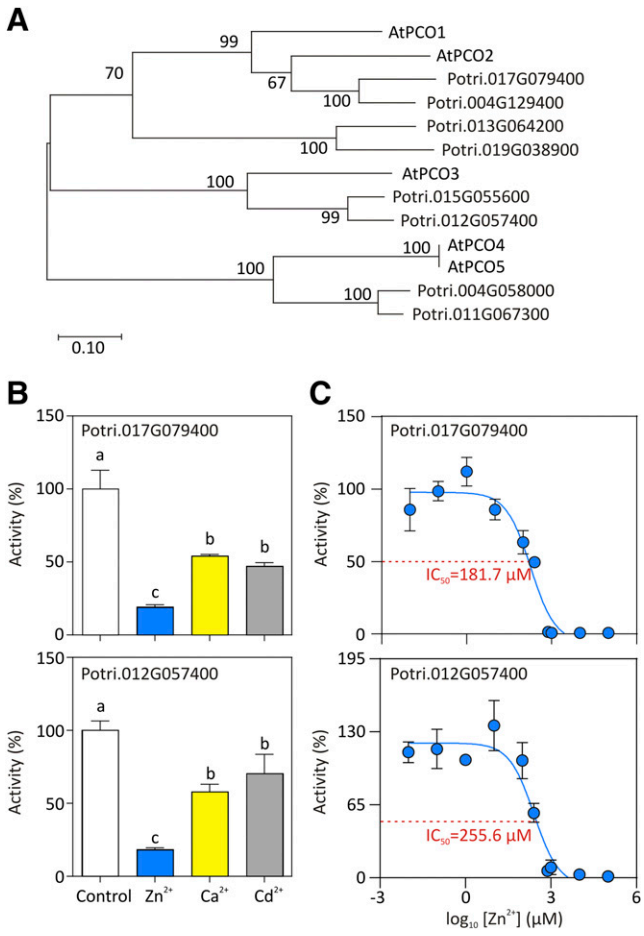

Figure 5. Zn^{2+} exerts an inhibitory effect on poplar PCOs in vitro. A, Phylogenetic tree of PCO proteins from Arabidopsis and *P. trichocarpa* generated from a multialignment processed via the maximum-likelihood algorithm. B, Activity inhibition of poplar PCOs Potri.012G057400 and Potri.017G079400 by different cations (Zn^{2+}, Ca^{2+}, and Cd^{2+}) using poplar Pop_ERFB2-1 14-amino acid N-terminal peptide as a substrate. Reactions were performed using 0.1 μM PCOs, 1 mM ERF, and 100 μM metals for 2 min. Data are presented as means ± SE (n = 3). Results were analyzed by one-way ANOVA followed by Tukey's posthoc test, and different letters indicate significant differences ($P < 0.05$). C, Zn^{2+} IC_{50} fitting curves for poplar Potri.012G057400 and Potri.017G079400 activity on Pop_ERFB2-1 14-amino acid N-terminal peptide. Zn^{2+} effect on PCOs is expressed as enzyme activity (%) compared with that in the control (100%). Reactions were performed using 0.2 μM PCOs for 2 min, and metal concentrations are indicated in logarithmic scale. Data are presented as means ± SE (n = 3).

the active sites. Although all three metals could inhibit PCO activity, Zn exhibited the strongest effect (Fig. 5B). Indeed, in the presence of 100 μM Zn, Potri.017G079400 and Potri.012G057400 activity was reduced by 81% and 82%, respectively. We also evaluated the extent of such inhibition, in terms of IC_{50} (half maximal inhibitory concentration) values (Fig. 5C). We measured the activity of the enzymes in the presence of a wide range of Zn concentrations from 10 nM to 100 mM, compared with that under control conditions (100% of activity). For both Potri.017G079400 and Potri.012G057400, the IC_{50} values were comparable at 181.7 and 255.6 μM, respectively. We therefore favored the hypothesis that Zn excess promotes ERF-VII stabilization and the consequent induction of anaerobic genes by inhibiting the oxidase enzymes that target these proteins for proteasomal degradation.

Zn Excess Mimics Fe Deficiency to Induce Hypoxia-Responsive Genes

Several genes involved in iron deficiency signaling and homeostasis, such as *Natural Resistance Associated Macrophage Protein1* (*NRAMP1*) and *NRAMP6*, *basic Helix-Loop-Helix* (*bHLH*)*038*, and *Zig Suppressor2 (ZIP2;* Ariani et al., 2015), responded to Zn stress in poplar (Fig. 1A). Since PCOs require Fe^{2+} to oxidize N-terminal Cys (White et al., 2018), we speculated that Zn excess may mimic iron starvation in vivo in terms of ERF-VII transcription factors. To test this hypothesis, we generated transgenic Arabidopsis plants that express the *RAP2.12$_{1-28}$-PpLuc* construct under the control of the 35S-Cauliflower mosaic virus promoter. Firefly luciferase activity was significantly stimulated in 5-d-old seedlings treated with 1 mM Zn for 72 h (Fig. 6A), confirming the results obtained with transiently transformed protoplasts (Fig. 4D). Moreover, Zn stress and hypoxia (1% [v/v] oxygen) exhibited the same inductive effect on the synthetic promoter *pHRPE* (Weits et al., 2019) in the roots of 10-d-old plants (Fig. 6B). Next, we tested whether iron starvation could stabilize ERF-VII proteins and indeed measured higher luciferase in iron-starved *RAP2.12$_{1-28}$-PpLuc* seedlings as compared with that in seedlings supplied with iron (Fig. 6C). Additionally, iron deficiency also induced higher expression of several hypoxia-responsive genes (Fig. 6D; Supplemental Table S5). Considered together, these results supported the hypothesis that ERF-VII transcription factors are stabilized when PCOs are inhibited by substrate (oxygen) or by cofactor (Fe^{2+}) shortage, the latter being caused by actual low iron levels or Zn competition.

ERF-VII-Responsive Genes Improve Tolerance to Zn Excess in Arabidopsis

Once we observed that Zn excess or iron starvation enhanced the expression of hypoxia-responsive genes through inhibiting PCO in poplar and Arabidopsis, we wondered whether ERF-VII activity provides

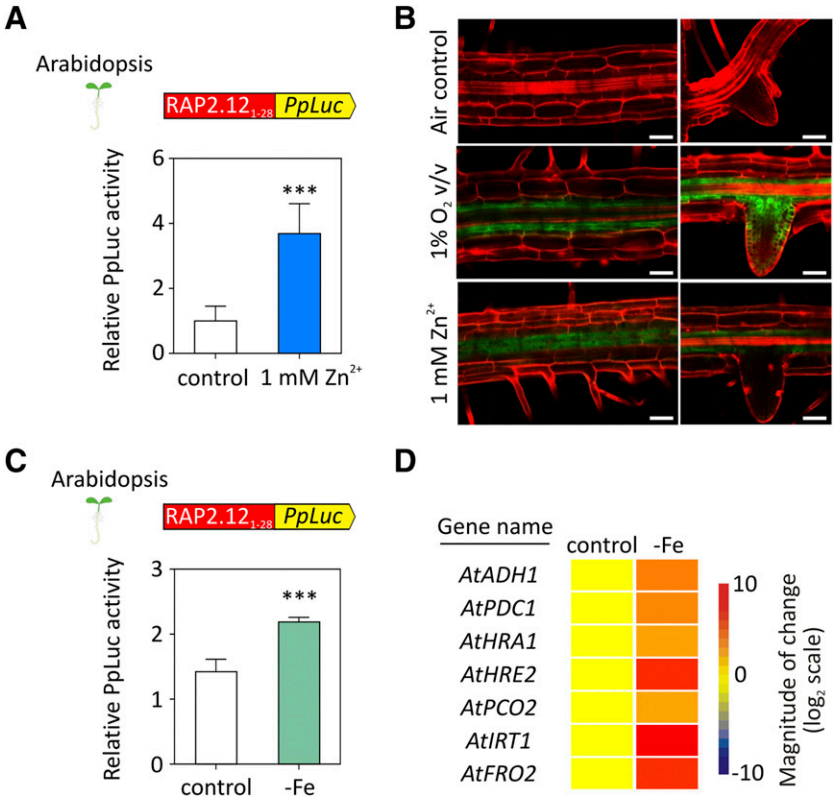

Figure 6. Zn excess and iron starvation similarly induce hypoxia-like responses in Arabidopsis. A, Effect of 1 mM Zn on PpLuc activity in 8-d-old Arabidopsis seedlings stably expressing the MC-degron reporter *RAP2.12$_{1-28}$-PpFluc* (Weits et al., 2014). Data are shown as means ± SD ($n = 5$); ***, $P < 0.01$, as assessed by two-tailed Student's *t* test. B, Laser-scanning confocal images of GFP driven by the hypoxia-responsive synthetic promoter HPRE (*pHRPE:GFP*) in Arabidopsis roots under control (Air control), hypoxia (1% [v/v] oxygen, 48 h), and Zn excess (1 mM $ZnSO_4$, 48 h). Bars = 100 μm. C, Effect of iron starvation on luciferase activity in 6-d-old *RAP2.12$_{1-28}$-PpFluc* transgenic seedlings. Data are shown as means ± SD ($n = 5$); ***, $P < 0.001$, as assessed by two-tailed Student's *t* test. D, Heat map showing relative expression of hypoxia and Zn excess marker genes in 6-d-old Arabidopsis Col-0 seedlings under control and iron-starvation conditions.

protection against Zn stress. Thus, we compared *erf-VII* mutant and wild-type seedlings after 3 d of Zn supplementation at different concentrations. Remarkably, the *erf-VII* mutant exhibited higher sensitivity to Zn, as also demonstrated by reduced growth and total chlorophyll accumulation (Fig. 7, A and B), which was accompanied by reduced expression of ERF-VII genes induced by Zn excess (Fig. 7C; Supplemental Table S6). These results support the idea that induction of hypoxia-responsive genes by ERF-VII also contributes to Zn tolerance, at least in Arabidopsis.

Zn Stress and Waterlogging Affect Poplar Fitness

Poplar trees can be used for phytoremediation of heavy metals in riparian areas, which are regularly subjected to flood events, since they are able to grow in waterlogged, and thereby hypoxic, soils (Isebrands and Richardson, 2014; Ciszewski and Grygar, 2016). Considering the molecular cross talk between Zn excess and hypoxia in this species, we were interested in monitoring the plant physiological response and fitness under the combination of Zn stress and waterlogging. We therefore subjected *P. alba* 'Villafranca' poplar plants for 4 and 10 d to four different hydroponic conditions: aerated control solution, Zn excess (1 mM $ZnSO_4$), waterlogging, and a combination of the two stresses. After 4 d, plants did not show any significant difference in terms of fresh and dry biomass as compared with that under the control condition (Supplemental Tables S7 and S8).

Conversely, after 10 d of growth in the conditions described above, Zn-stressed and waterlogged plants displayed a similar symptomatic phenotype when compared with that of control plants, specifically chlorosis in the younger leaves and reduced growth (Fig. 8A). We therefore quantified the chlorotic phenotype in terms of total chlorophyll content (SPAD units), which revealed a significant decrease in chlorophyll under all three stress conditions as compared with that in the control (Fig. 8B). Ten days of treatment caused a decrease in total biomass compared with that in the controls, as shown by a significant decrease in fresh weight (Fig. 8C; Supplemental Table S9) followed by the same trend in dry weight, albeit this result was not significant (Fig. 8D; Supplemental Table S10).

These results prompted us toward two main speculations. First, both Zn excess and waterlogging exert a similar repressive effect on poplar growth and thereby possibly impact on similar molecular mechanisms. Moreover, since the combination of the two stresses did not impair biomass production and chlorophyll

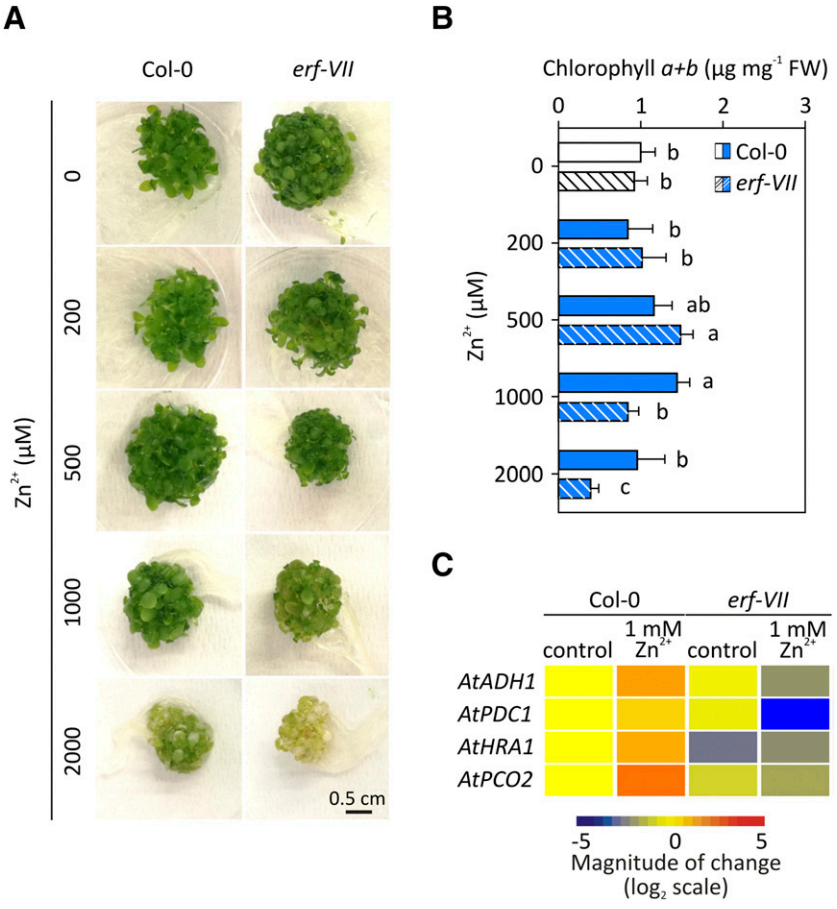

Figure 7. ERF-VIIs contribute to Arabidopsis tolerance to Zn excess. A, Five-day-old wild-type and *erf-VII* Arabidopsis seedlings were subjected to a range of Zn concentrations (from 0 to 2,000 µM) for 3 d. Photographs were taken at the end of the treatments and show a representative sample for each treatment. Bar = 0.5 cm. B, Total chlorophyll quantification in wild-type and *erf-VII* seedlings at the end of the treatment described in A. Data are presented as means ± SD ($n = 6$). Different letters indicate statistically significant differences ($P < 0.05$, as assessed by two-way ANOVA followed by the Holm-Sidak posthoc test). FW, Fresh weight. C, Heat map displaying differential expression of hypoxia marker genes in response to 1 mM Zn in wild-type and *erf-VII* seedlings at the end of the treatments as described in A.

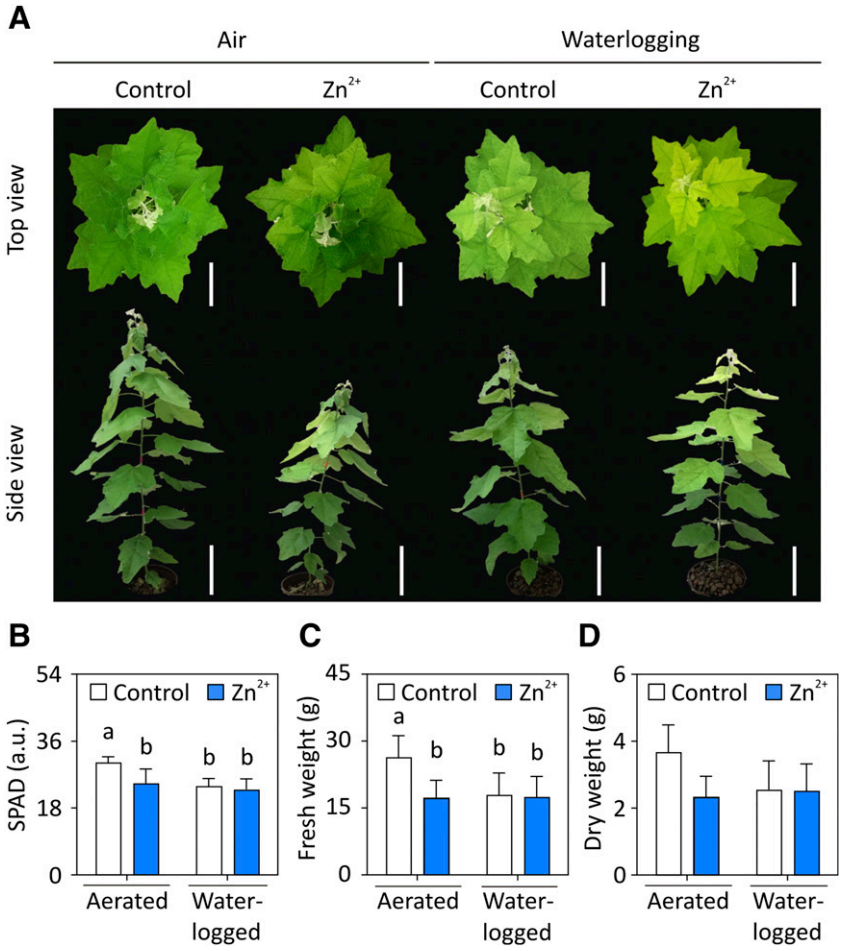

Figure 8. Effects of waterlogging and Zn stress on poplar phenotype. A, 'Villafranca' poplars were subjected to 1 mM $ZnSO_4$ stress, to waterlogging, and to a combination of the two for 10 d. Photographs were taken at the end of the treatments and show a top view and a side view of a representative plant for each treatment. Images of different plants were digitally extracted and combined for comparison. Bars = 15 cm. B, Total chlorophyll (SPAD units) in leaves at the end of 10 d of the treatments described in A. Data are presented as means ± SD ($n = 10$). C, Fresh weight of the total biomass of plants after 10 d of the treatments described in A. Data are presented as means ± SD ($n = 5$). D, Dry weight of the total biomass of plants after 10 d of the treatments described in A. Data are presented as means ± SD ($n = 5$). For B and C, different letters indicate statistically significant differences as assessed by two-way ANOVA followed by the Holm-Sidak posthoc test ($P < 0.05$).

accumulation more than each single treatment, the reduction in growth rate could be considered as an adaptive strategy to cope with unfavorable environmental conditions.

Waterlogging Affects Zn Accumulation in Poplar Roots

Once we established that root hypoxia and Zn excess share similarities in their phenotypic adaptations as well as in the molecular response, we tested whether waterlogging may impact on Zn accumulation and thereby affect the performance of the Zn-tolerant poplar 'Villafranca' clone in phytoremediation. Leaves and root tissues were collected from plants subjected to the growth conditions described above to evaluate their Zn content. As expected from the phenotypes described above (Fig. 8), substantial Zn accumulation occurred after 10 d in plants subjected to Zn treatment both under aerated and waterlogged conditions (Fig. 9). However, we recorded a significant reduction of Zn levels in the roots of Zn-treated plants when these were also subjected to waterlogging, as compared with that resulting from Zn treatment under aerated conditions. Surprisingly, such an effect of waterlogging on Zn accumulation was not detected in the leaves (Fig. 9A), despite the likely occurrence of ATP shortage under waterlogging (Gibbs and Greenway, 2003), which would have been expected to impact on the active loading of Zn into the xylem and thereby on its distribution to the shoot (Olsen and Palmgren, 2014). Nevertheless, in agreement with the reduced radical accumulation of Zn, we detected a significant reduction in the expression of genes involved in metal acquisition and transport in root tissues under waterlogged conditions (Fig. 9B; Supplemental Table S11). Among these, *Nicotianamine Synthase4* (*Pop_NAS4*) contributes to the production of nonproteinogenic amino acid that chelates cations to facilitate their uptake in the roots and their translocation through the vessels (Schuler and Bauer, 2011; Tsednee et al., 2014). On the other hand, *Pop_ZIP4.2* encodes for a membrane Zn transporter, whereas *Pop_CAX1.2* and *Pop_MTP1.1* encode for two vacuolar $Zn\text{-}H^+$ antiporters. We speculated that under waterlogging, the plants reduced root Zn accumulation by decreasing the Zn uptake (via Pop_ZIP4.2 and nicotianamine chelation) and limiting its compartmentalization into the vacuole (via Pop_CAX1.2 and Pop_MTP1.1). Taken together, these results suggested that poplar can fine-tune Zn uptake in the root to cope with unfavorable soil conditions, such as waterlogging.

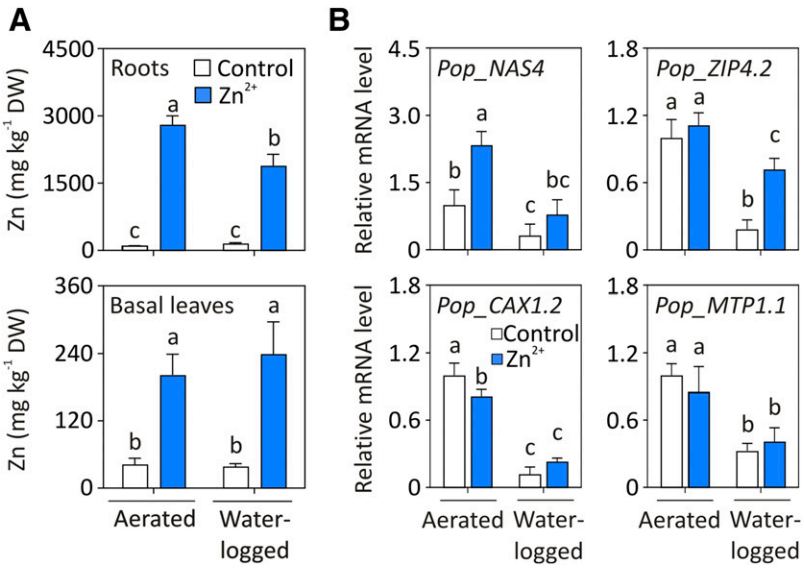

Figure 9. Zn uptake decreases in roots under waterlogging. A, Zn concentration (mg kg^{-1} dry weight [DW]) in poplar roots and basal leaves after 10 d of treatment of 1 mM $ZnSO_4$ stress, waterlogging, and a combination of the two. B, Relative expression levels of Zn transporters in poplar roots after 10 d of the treatments: *Pop_NAS4* (*Potri.004G193400*), *Pop_ZIP4.2* (*Potri.001G160400*), *Pop_CAX1.2* (*Potri.009G045800*), and *Pop_MTP1.1* (*Potri.014G106200*). All data are presented as means ± SD ($n = 5$). Different letters indicate statistically significant differences as assessed by two-way ANOVA followed by the Holm-Sidak posthoc test ($P < 0.05$).

DISCUSSION

In this work, we investigated the convergence of molecular and physiological responses of poplar trees to Zn excess and waterlogging and proceeded to examine the adaptation to the combination of these two stresses. So far, this aspect has remained overlooked, despite its relevance for soil Zn remediation and poplar physiology. Indeed, the recently increased frequency of flooding events intensifies the probability that contaminants, including metals, are remobilized from the river banks to the surrounding riparian areas (Ciszewski and Grygar, 2016). For this reason, phytoremediation of these areas has focused on employing plant species that thrive in naturally flooded areas and tolerate high amounts of metals, such as poplars (Pilon-Smits, 2005; Müller et al., 2013).

By comparing the transcriptional responses of poplar roots to Zn stress (Ariani et al., 2015) and waterlogging (Kreuzwieser et al., 2009), we observed a remarkable overlap between Zn-regulated genes and hypoxia-responsive ones. The hypoxia-like response activated under Zn stress appeared to be part of the adaptive response of the plants to Zn stress, rather than being induced by an actual reduction in oxygen availability in the roots, in response to Zn excess (Fig. 1). The similarity between these responses was conserved irrespective of the Zn tolerance of the poplar variety, as demonstrated by its occurrence in two poplar cultivars characterized by different sensitivity to Zn stress (Fig. 2; Romeo et al., 2014).

In Arabidopsis, the transcriptional response to hypoxia is regulated mainly by the ERF-VII transcription factors RAP2.2 and RAP2.12, whose aerobic instability is ensured by the N-degron pathway (van Dongen and Licausi, 2015). Additional control by light, potassium, and sugar availability has been reported to impact on the stability and activity of these proteins (Abbas et al., 2015; Shahzad et al., 2016; Loreti et al., 2018). Unbalanced metal homeostasis is likely to directly or indirectly affect these regulatory pathways. In this study, we focused on the control exerted by PCOs, responsible for the oxidation of the Cys in the second position of the ERF-VIIs that precedes their degradation (Weits et al., 2014). PCOs were recently shown to require molecular oxygen and Fe^{2+} to oxidize the Cys (White et al., 2017, 2018). Interestingly, we observed that divalent cations were able to inhibit the enzyme activity in vitro, and Zn^{2+} was especially effective in this regard (Fig. 5). We therefore speculated that Zn^{2+} may also outcompete Fe^{2+} for PCO binding in vivo. Indeed, prolonged iron starvation also caused stabilization of an ERF-VII reporter and induced hypoxia-responsive genes in Arabidopsis seedlings (Fig. 6, C and D). This is in agreement with the transcriptional response of Arabidopsis roots to 2 d of iron limitation reported by Dinneny et al. (2008). The very high Zn concentrations required for PCO inactivation in vitro, in the micromolar range, induced us to question the physiological relevance of this phenomenon. On the one hand, the activity of other enzymes, such as Carboxypeptidase A and Kallikreins, has been shown to be inhibited at similar metal concentrations (Maret, 2013). On the other hand, cytosolic and nuclear Zn levels of poplar root cells exposed to Zn excess in the soil are still unknown. Pioneering endeavors in assessing subcellular Zn^{2+} levels through a genetically encoded Förster resonance energy transfer-based sensor have been conducted using Arabidopsis root cells, although the saturation of the sensor did not allow the detection of Zn concentrations above the nanomolar range (Lanquar et al., 2014). However, in balanced nutrient conditions, Arabidopsis mesophyll vacuoles contain Zn in the micromolar range (Lanquar et al., 2010). Considering that soil Zn content reaches levels up to thousands mg kg^{-1} in contaminated soils (Long et al., 2003), it is not unlikely that the intracellular concentration of this metal in root cells may reach the concentrations

compatible with PCO inhibition. It is also worth considering that prolonged exposure to Zn excess was necessary to activate the hypoxia-like response in poplar roots, since Zn supplementation for 4 h was unable to activate the ERF-VII reporter in protoplasts (Fig. 4). We therefore speculate that PCO enzymes might be especially sensitive to Zn inactivation during their biogenesis at the time when the metal ion is incorporated. During chronic exposure to Zn excess, such as in our experimental conditions, this would lead to the accumulation of inactive PCOs over time.

Despite acting as a cofactor or structural element for several proteins, Zn^{2+} represents a threat to many iron-containing enzymes. Indeed, among biogenic metal species characterized by positive divalent charge and ionic radius similar to iron, Zn possesses higher ligand-coordinating strength according to the series of Irving and Williams (1948) and is therefore likely to form more stable complexes. In light of this, despite metalloproteins having evolved to preferentially accommodate the cognate cation that ensures their biological function and to protect the binding sites from the attack of undesired metal contenders, Zn can easily displace and substitute iron (Dudev and Nikolova, 2016). It is therefore the responsibility of the cell machinery to maintain Zn homeostasis at a level that prevents competition with Fe^{2+}. In this regard, the inactivation of poplar PCO enzymes at cellular Zn concentrations below or in the proximity of toxic levels, as demonstrated by the survival and limited reduction in the growth rate (Fig. 8), is surprising: this specific molecular mechanism is rather Zn sensitive for a plant species able to accumulate high intracellular Zn levels (Sebastiani et al., 2014). Thus, we speculated that this enzymatic sensitivity to moderate Zn levels might rather have a signaling function in poplar, via ERF-VIIs or other transcription factors controlled by the N-degron pathway.

Induction of ERF-VII-regulated genes appeared to be beneficial for the tolerance of Zn excess in Arabidopsis (Fig. 7). Future studies should be aimed at understanding whether the whole anaerobic response is required for Zn tolerance or if some genes play a major role.

Additional mechanisms may be activated by Zn or low iron-induced inactivation of PCOs. Four bHLH transcription factors, namely bHLH38/bHLH39/bHLH100/bHLH101, have been identified as being involved in iron sensing in Arabidopsis (Sivitz et al., 2012). All four bHLHs are characterized by a conserved Cys residue in the penultimate position that makes them potential N-degron substrates. Poplar orthologs of these genes are also transcriptionally up-regulated in response to Zn excess, suggesting their potential involvement in the adaptive response to this stress (Ariani et al., 2015). Future experimental efforts may be aimed at addressing whether posttranslational stabilization via PCO inhibition is involved in the induction of their activity. Moreover, the involvement of MC proteins in the response to Zn excess and iron deficiency might suggest a common evolution of nutrient homeostasis mechanisms that over time diverged into the ERF-VII and bHLH families.

As mentioned before, the inhibition of PCO activity under limiting oxygen conditions has been associated with the up-regulation of hypoxia-related genes via the stabilization of ERF-VII (Weits et al., 2014). Here, we observed that Pop_ERFB2-1, a close RAP2.12/RAP2 ortholog in poplar, is able to activate hypoxia-responsive genes (Fig. 3). In agreement with the proposed inactivation of PCO activity by Zn, this transcription factor is stabilized by Zn excess at normoxic oxygen levels (Fig. 4). Despite the high sequence similarity between RAP2.12 and Pop_ERFB2-1, the latter failed to restore the molecular response to anaerobiosis in the Arabidopsis pentuple *erf-VII* mutant (Fig. 3). This could be explained by small differences in the amino acid sequences between the two ERF-VIIs that hindered or altered the interaction of Pop_ERFB2-1 with the Arabidopsis ERF-VII partners that enable recruitment of the transcriptional complex on the promoters of target genes. Moreover, RAP2.12 was unable to activate anaerobic genes when transiently expressed in poplar protoplasts (Fig. 3E). Previous protein interaction surveys identified ERF-VII interactors involved in transcriptional regulation in Arabidopsis: RAP2.2 was shown to bind to the Mediator complex subunit Med25, which likely serves as a scaffold for the assembly of RNA polymerase II and general transcription factors, and the chromatin-remodeling ATPase BRAHMA (Ou et al., 2011; Vicente et al., 2017). Additionally, interaction with transcription factors belonging to different protein families, which may mediate binding to additional targets under specific conditions, was also reported (Lumba et al., 2014). The failure of PpSPAb or OsSPA1 from *Physcomitrella patens* and rice (*Oryza sativa*), respectively, to complement the light-sensing negative regulator *spa* Arabidopsis mutant (Ranjan et al., 2014) is another example of the interaction specificity required for a transcription factor to exert its function.

The overlap between the transcriptional response to Zn and low oxygen observed in poplar is of great interest, since these species are not unlikely to experience a combination of these two stresses for the reasons mentioned above. Remarkably, 10 d of 1 mM Zn supplementation or waterlogging exerted a similar effect on the tolerant *P. alba* 'Villafranca'. Both treatments reduced biomass accumulation with concomitant chlorosis of the younger leaves (Fig. 8). The apparent discrepancy with the previously reported absence of toxicity symptoms in the 'Villafranca' plants exposed to 1 mM Zn (Romeo et al., 2014) is likely explained by the different anion used in our experimental conditions: $ZnSO_4$ instead of $Zn(NO_3)_2$. Additionally, we put forward two explanations for the observed toxic effect of Zn. First, this metal could compete with iron to be taken up in the roots via low-affinity transporters, such as IRT1 (Sinclair and Krämer, 2012). Consequently, Zn-induced iron starvation might repress chlorophyll

biosynthesis, since heme synthesis requires iron and Zn is likely to replace Mg^{2+} in the porphyrin ring (Tripathy and Pattanayak, 2012). Alternatively, stabilized ERF-VII proteins, induced by either Zn excess or waterlogging, could be involved in active repression of chlorophyll biosynthetic genes, as reported by Abbas et al. (2015).

Since the combination of Zn excess and waterlogging did not enhance leaf chlorosis and biomass reduction as compared with that resulting from the single stresses (Fig. 8), we concluded that the two environmental cues impact to the same extent on these regulatory and biosynthetic pathways. Instead, we observed a decrease in Zn accumulation in poplar roots under Zn stress and waterlogging, compared with that under Zn excess, concomitant with the repression of genes involved in Zn uptake and vacuolar compartmentalization (Fig. 9). This can be interpreted as a conservative strategy to limit Zn accumulation before it reaches toxic cellular concentrations when the plant metabolism is already dedicated to coping with oxygen deficiency at the root level.

In conclusion, in this work, we shed new light on the cross talk in the molecular and physiological responses of poplars to two environmental stresses: Zn excess and waterlogging. From a phytoremediation perspective, understanding the adaptive responses of plants to this specific combination of environmental cues is fundamental to identify agronomic practices and breeding strategies that will make this approach more effective, reliable, and widely applicable.

MATERIALS AND METHODS

Plant Material and Growth Conditions

Plantlets of *Populus alba* 'Villafranca' clone were maintained in in vitro conditions in Magenta vessels on 0.7% (w/v) agar woody plant medium at pH 5.7 (Lloyd and McCown, 1980). Four-week-old plantlets, derived from in vitro culture (one-half-strength woody plant medium), were transferred to pots filled with perlite (Laterlite) and closed in plexiglass boxes to maintain 100% humidity. The plantlets were acclimatized for 4 weeks under controlled environmental conditions (23°C/18°C day/night temperature, 65% to 70% relative humidity, and 16-h photoperiod at a photosynthetic photon flux density of 400 μmol m^{-2} s^{-1} supplied by fluorescent lights). Hoagland solution (Arnon and Hoagland, 1940) was supplied as a nutrient solution, and relative humidity was gradually reduced from 100% to 65% to 70%. After the acclimation period, plants were transferred into plastic pots containing 4 to 8 mm diameter expanded Agrileca clay (Laterlite) and grown in Hoagland solution with continuous aeration by aquarium pumps (250 L h^{-1}).

Woody cuttings of 'Villafranca' and *Populus* × *canadensis* 'I-214' clone were provided by Centro di Ricerche Agro-Ambientali Enrico Avanzi. After rooting, cuttings were transferred into plastic pots, containing 4 to 8 mm diameter expanded Agrileca clay (Laterlite), and acclimated to a hydroponic system under controlled environmental conditions, as described before. At the end of the acclimation process, plants were pruned and maintained at unique stem growth.

Seeds of the Arabidopsis (*Arabidopsis thaliana*) *erf-VII* mutant, described by Abbas et al. (2015), were provided by Michael Holdsworth. Seeds of *prt6-5* (SALK_051088) and *ate1 ate2* mutants were previously described by Gibbs et al. (2011) and Licausi et al. (2011), respectively. The Col-0 ecotype was used as a wild-type reference. Arabidopsis seeds were sown in moist soil, stratified at 4°C in the dark for 48 h, and germinated at 22°C/18°C day/night with a 16-h photoperiod. For in vitro seedling cultivation, seeds were sterilized and, subsequently, germinated in 2 mL of liquid one-half-strength Murashige and Skoog (MS) medium (Murashige and Skoog, 1962) supplemented with 1% (w/v) Suc (Duchefa), on six-well plates (Euroclone) with shaking at 90 rpm.

Cloning of the Various Constructs

The full CDS of the closest Arabidopsis *RAP2.12* gene (*At1g53910*) homolog in poplar (*Potri.003G071700*, named *PtERFB2-1* according to Zhuang et al. [2008]) was cloned from *P. alba* 'Villafranca' using Phusion High Fidelity DNA-Polymerase (New England Biolabs) with primers designed on the *Populus trichocarpa* genome. The high similarities between 'Villafranca' (*Pop_ERFB2-1*) and *P. trichocarpa* (*PtERFB2-1*) sequences at the nucleotide and amino acid levels are shown in Supplemental File S3.

The *Pop_ERFB2-1* amplicon was cloned into *pENTR/D-TOPO* (Life Technologies) and then recombined into *p2GW7*, *p2GWL7*, and *pGWB514* (Life Technologies) destination vectors using the LR reaction mix II (Life Technologies).

The CDSs of two 'Villafranca' poplar *PCOs* (*Potri.012g057400* and *Potri.017g079400*) were isolated using primers designed on the *P. trichocarpa* genome and carrying *Nde*I and *Xho*I sites at the 5′ ends of forward and reverse primers, respectively. The *Nde*I/*Xho*I fragments were ligated into *pET28a(+)* vector, suitable for protein expression and purification through an N-terminal His_6 tag. All the primers used for cloning of the described fragments are listed in Supplemental Table S12.

Luciferase Transactivation and Protein Stability Assay

'I-214' mesophyll protoplasts were isolated and transfected according to Yoo et al. (2007). Two and a half micrograms of each plasmid was used to transfect 100 μL of protoplasts in suspension. After overnight incubation in the dark at 23°C, the firefly (*Photinus pyralis*) luciferase activity was measured and normalized with the sea pansy (*Renilla reniformis*) luciferase signal (PpLuc/RrLuc) using the Dual-Luciferase Reporter Assay System (Promega) according to the manufacturer's protocol. For each sample, five independent replicates were used.

Low-Oxygen and Zn Treatments

After 10 d of hydroponic solution, woody cuttings of poplar plants were randomized in groups of five plants and subjected to the following treatments. 'Villafranca' and 'I-214' cuttings were treated with 1 mM $ZnSO_4$ (1 μM as a control) for 21 d. The total amount of $ZnSO_4$ given in 21 d was 0.78 g per plant. 'Villafranca' poplars acclimated in vitro, instead, were treated with 1 mM $ZnSO_4$ (1 μM as a control), waterlogging, or a combination of the two stresses for 4 or 10 d. The total amount of $ZnSO_4$ given in 10 d was 0.43 g per plant.

Poplar mesophyll protoplasts were incubated overnight with different concentrations of $ZnSO_4$ (0, 100, 200, 400, and 800 μM) dissolved in WI solution (0.5 mM mannitol, 4 mM MES-KOH at pH 5.7, and 20 mM KCl).

Four-day-old Arabidopsis seedlings were subjected to a 6-h partial submergence treatment provided by the addition of 3 mL of fresh one-half-strength MS (1% [w/v] Suc) in the dark to avoid oxygen release by photosynthesis, without shaking. Control seedlings were kept in the dark under shaking conditions.

Five-day-old Arabidopsis seedlings cultivated on liquid one-half-strength MS, supplemented with 1% (w/v) Suc, were transferred to control medium (0 μM $ZnSO_4$) or to medium supplemented with $ZnSO_4$ (200, 500, 1,000, or 2,000 μM) for 3 d.

For confocal microscopy observations, 7-d-old Arabidopsis seedlings were grown on square plastic plates (12-cm sides) containing 50 mL of one-half-strength MS, supplemented with 1% (w/v) Suc and 0.8% (w/v) plant agar. Subsequently, plates were treated with 1% (v/v) oxygen for 6 h or with 1 mM $ZnSO_4$, dripped on the root surface, for 48 h.

Germination under Iron-Starvation Conditions

Arabidopsis seeds were germinated and grown for 6 d under control (one-half-strength MS containing 50 μM FeNaEDTA and supplemented with 1% [w/v] Suc) or iron starvation (one-half-strength MS, 0 μM FeNaEDTA, and 1% [w/v] Suc) conditions.

Oxygen Measurement

Molecular oxygen measurements in hydroponic solution were performed through the optical oxygen meter FireStingO2 (PyroScience), using the OXF500PT fiber-optic micro sensor, according to the manufacturer's protocol.

Chlorophyll Quantification

The relative chlorophyll concentrations were estimated using a SPAD-502 chlorophyll meter (Minolta) on 10 fully expanded 'Villafranca' poplar leaves randomly selected among the four treatments after 10 d of the Zn and waterlogging combined experiment.

Eight-day-old Col-0 and *erf-VII* Arabidopsis seedlings were frozen and ground, and the resulting powder was incubated with 100% (v/v) methanol overnight at 4°C in the dark. After centrifugation, the supernatant was separated from the pellet and the absorbance of the extract was spectrophotometrically measured at 665.2 and 652.4 nm. Chlorophyll concentrations were calculated according to Lichtenthaler (1987).

Zn Concentration Analysis in Poplar

The total concentration of Zn in poplar dry root and leaf, after 4 or 10 d, was determined after digestion with concentrated nitric acid (HNO_3) by atomic absorption spectrophotometry (model 373; PerkinElmer). One analytical reference standard of Zn was used as a control (WEPAL IPE; Wageningen University).

Plant Transformation and Genotyping

Arabidopsis *erf-VII* stable transgenic plants were obtained using the floral dip method (Clough and Bent, 1998). T0 seeds were screened for hygromycin resistance; two independent transgenic lines were identified (*35S:Pop_ERFB2-1* lines #2 and #3), and the presence of *Pop_ERFB2-1* cDNA was tested via PCR using GoTaq DNA polymerase (Promega) using the primers listed in Supplemental Table S12.

Identification of Poplar PCOs

Identification of PCO protein sequences in *P. trichocarpa* was performed by searching the Phytozome database (www.phytozome.net) using the BLAST algorithm (Altschul et al., 1990) and Arabidopsis PCO1 (At5g15120) as a query. The obtained proteins were then aligned back against the Arabidopsis protein database to ensure that they represent the closest homologs of AtPCOs.

Phylogenetic Analysis

Phylogenetic analysis was performed using MEGAX (Kumar et al., 2018). The phylogenetic trees were obtained aligning Arabidopsis and poplar PCOs and ERF-VIIs using the MUSCLE algorithm (Edgar, 2004). The maximum-likelihood method was applied to build the phylogenetic trees, using a bootstrapping method based on 100 replicates.

PCO Purification and in Vitro Inhibition Assay

P. alba 'Villafranca' PCOs (Potri.012g057400 and Potri.017g079400) were purified using Ni^{2+} affinity chromatography, following the protocol described by White et al. (2018). Cys oxidation activity of PCOs was measured toward a 14-amino acid peptide (ERFB2-$1_{2\text{-}16}$, H_2N-CGGAIISDFIAPTT-COOH), corresponding to the N terminus of PtERFB2-1 protein (Potri.003G071700). The metal inhibition assays were performed in 30 μL of buffer: 20 mM NaCl, 20 mM HEPES, 1 mM tris(2-carboxyethyl)phosphine, and 1 mM L-ascorbic acid, at pH 7.5. Buffer was supplemented with 25 nM enzyme, 1 mM substrate, and 1 mM inhibitor ($ZnCl_2$, $CaCl_2$, or $CdCl_2$). The reactions were run for 1.5 min at 25°C and stopped by quenching 5 μL in 45 μL of 1% (v/v) formic acid.

For the Zn IC_{50} assays, a wide range of Zn^{2+} ($ZnCl_2$) concentrations (10 nM, 100 nM, 1 μM, 10 μM, 100 μM, 250 μM, 750 μM, 1 mM, 10 mM, and 100 mM) were tested. The enzymes were incubated on ice with the metal for 30 min before performing the reactions for 2 min. All the samples were analyzed by HPLC coupled with quadrupole-time of flight-mass spectrometry (Xevo G2-XS QTof) as previously described by White et al. (2018).

RNA Extraction and RT-qPCR Analysis

Poplar total RNA was isolated from 80 to 100 mg of frozen and ground roots using the Spectrum Plant Total RNA Kit (Sigma-Aldrich), according to the manufacturer's protocol.

For Arabidopsis RNA extraction, a phenol-chloroform extraction protocol was employed, as described by Weits et al. (2014). One microgram of RNA was subjected to DNase treatment along with cDNA synthesis, both performed with the Maxima First Strand cDNA Synthesis Kit for RT-qPCR with dsDNase (Thermo Scientific).

qPCR was carried out with the ABI Prism 7900 sequence detection system (Thermo Scientific), using the SYBR Green PCR Master Mix (Thermo Scientific).

UBIQUITIN10 (*At4g05320*) and *β-Tubulin* (*Potri.011G162500*) were used as housekeeping genes for Arabidopsis and poplar samples, respectively. All poplar primers were designed on the *P. trichocarpa* genome, and the primer sequences for the genes analyzed are listed in Supplemental Table S13.

Relative quantification of the expression of each gene was performed using the comparative threshold cycle method as described by Livak and Schmittgen (2001). Two technical replicates were used for each of the five biological samples, and the data are representative of at least two independent experiments giving comparable profiles.

Confocal Imaging

Roots of 7-d-old seedlings were observed with the 20× objective of an Olympus FluoView1000 inverted confocal microscope. GFP fluorescence was excited with 488-nm laser light (laser transmissivity, −6%; photomultiplier voltage, 650 V) and collected between 495 and 540 nm with a long-pass emission filter. Propidium iodide stain marking plant cell walls was excited at 488 nm (laser transmissivity, −6%; photomultiplier voltage, 550 V) and collected at 590 to 680 nm. Scanner and detector settings were kept unchanged during the whole experiment. Images were analyzed with the Olympus FluoView FV1000 software.

Statistical Analysis

Statistical analysis was performed using GraphPad Prism version 6.00. According to the data sets, Student's *t* test and one-way or two-way ANOVA were conducted, and differences between means were considered significant at $P < 0.05$. In one-way ANOVA, the multiple comparisons of means were performed with Tukey's method, whereas in two-way ANOVA, they were performed via the Holm-Sidak method.

Accession Numbers

The CDS of *ERFB2-1* from *P. alba* 'Villafranca' clone reported in this article can be found in the GenBank data libraries under accession number MK814744. All other Arabidopsis or poplar sequences can be retrieved from the Phytozome database (https://phytozome.jgi.doe.gov/pz/portal.html).

Supplemental Data

The following supplemental materials are available.

Supplemental Figure S1. Core hypoxia-responsive genes are responsive to low oxygen in poplar.

Supplemental Figure S2. Occurrence of common motifs in poplar and Arabidopsis ERF-VII proteins.

Supplemental Figure S3. Identification of the HRPE in the promoter of poplar hypoxia-responsive genes.

Supplemental Figure S4. Transcriptional regulation of *Pop_ERFB2-1* under Zn stress.

Supplemental Table S1. List of differentially expressed genes in poplar or Arabidopsis under Zn excess and low-oxygen conditions.

Supplemental Table S2. List of hypoxia-affected genes identified under Zn excess.

Supplemental Table S3. List of core hypoxia-responsive genes affected by Zn excess.

Supplemental Table S4. Transcriptional regulation of poplar ERF-VIIs under anoxia.

Supplemental Table S5. Transcriptional regulation of Arabidopsis hypoxia-responsive genes after 6 d of germination of Col-0 seeds, under iron starvation conditions.

Supplemental Table S6. Transcriptional regulation of Arabidopsis hypoxia-responsive genes under control and 1 mM Zn conditions for 2 d, in Col-0 and *erf-VII* mutant plants.

Supplemental Table S7. Fresh weight of *P. alba* 'Villafranca' plants under control, 1 mM Zn, waterlogging, and a combination of 1 mM Zn and waterlogging conditions, for 4 d.

Supplemental Table S8. Dry weight of *P. alba* 'Villafranca' plants under control, 1 mM Zn, waterlogging, and a combination of 1 mM Zn and waterlogging conditions, for 4 d.

Supplemental Table S9. Fresh weight of *P. alba* 'Villafranca' plants under control, 1 mM Zn, waterlogging, and a combination of 1 mM Zn and waterlogging conditions, for 10 d.

Supplemental Table S10. Dry weight of *P. alba* 'Villafranca' plants under control, 1 mM Zn, waterlogging, and a combination of 1 mM Zn and waterlogging conditions, for 10 d.

Supplemental Table S11. Relative expression levels of metal transporters in poplar roots under Zn stress and waterlogging conditions.

Supplemental Table S12. List of forward (5′→3′) and reverse (5′→3′) primer sequences for poplar CDS cloning.

Supplemental Table S13. List of forward (5′→3′) and reverse (5′→3′) primer sequences for poplar and Arabidopsis RT-qPCR analysis.

Supplemental File S1. Alignment of Arabidopsis and poplar ERF-VII proteins.

Supplemental File S2. Alignment of Arabidopsis and poplar PCO proteins.

Supplemental File S3. Protein alignment of ERFB2-1 in *P. trichocarpa* and *P. alba* 'Villafranca'.

ACKNOWLEDGMENTS

We thank Cristina Ghelardi and Francesca Vannucchi for assistance with poplar cultivation and Gaia Monteforti for sharing her expertise in atomic absorption spectrophotometry.

Received November 27, 2018; accepted April 12, 2019; published April 24, 2019.

LITERATURE CITED

Abbas M, Berckhan S, Rooney DJ, Gibbs DJ, Vicente Conde J, Sousa Correia C, Bassel GW, Marín-de la Rosa N, León J, Alabadí D, et al (2015) Oxygen sensing coordinates photomorphogenesis to facilitate seedling survival. Curr Biol **25:** 1483–1488

Abdullah AS (2015) Zinc availability and dynamics in the transition from flooded to aerobic rice cultivation. Journal of Plant Biology & Soil Health **2:** 1–5

Altschul SF, Gish W, Miller W, Myers EW, Lipman DJ (1990) Basic local alignment search tool. J Mol Biol **215:** 403–410

Ariani A, Di Baccio D, Romeo S, Lombardi L, Andreucci A, Lux A, Horner DS, Sebastiani L (2015) RNA sequencing of *Populus* × *canadensis* roots identifies key molecular mechanisms underlying physiological adaption to excess zinc. PLoS ONE **10:** e0117571

Arnon DI, Hoagland DR (1940) Crop production in artificial culture solutions and in soils with special reference to factors influencing yields and absorption of inorganic nutrients. Soil Sci **50:** 463–485

Banti V, Giuntoli B, Gonzali S, Loreti E, Magneschi L, Novi G, Paparelli E, Parlanti S, Pucciariello C, Santaniello A, et al (2013) Low oxygen response mechanisms in green organisms. Int J Mol Sci **14:** 4734–4761

Bouain N, Shahzad Z, Rouached A, Khan GA, Berthomieu P, Abdelly C, Poirier Y, Rouached H (2014) Phosphate and zinc transport and signalling in plants: Toward a better understanding of their homeostasis interaction. J Exp Bot **65:** 5725–5741

Broadley MR, White PJ, Hammond JP, Zelko I, Lux A (2007) Zinc in plants. New Phytol **173:** 677–702

Bui LT, Giuntoli B, Kosmacz M, Parlanti S, Licausi F (2015) Constitutively expressed ERF-VII transcription factors redundantly activate the core anaerobic response in *Arabidopsis thaliana*. Plant Sci **236:** 37–43

Ciszewski D, Grygar TM (2016) A review of flood-related storage and remobilization of heavy metal pollutants in river systems. Water Air Soil Pollut **227:** 239

Clough SJ, Bent AF (1998) Floral dip: A simplified method for Agrobacterium-mediated transformation of *Arabidopsis thaliana*. Plant J **16:** 735–743

Coleman JE (1998) Zinc enzymes. Curr Opin Chem Biol **2:** 222–234

Di Baccio D, Tognetti R, Sebastiani L, Vitagliano C (2003) Responses of *Populus deltoides* × *Populus nigra* (*Populus* × *euramericana*) clone I-214 to high zinc concentrations. New Phytol **159:** 443–452

Di Baccio D, Kopriva S, Sebastiani L, Rennenberg H (2005) Does glutathione metabolism have a role in the defence of poplar against zinc excess? New Phytol **167:** 73–80

Di Baccio D, Tognetti R, Minnocci A, Sebastiani L (2009) Responses of the *Populus* × *euramericana* clone I-214 to excess zinc: Carbon assimilation, structural modifications, metal distribution and cellular localization. Environ Exp Bot **67:** 153–163

Dinneny JR, Long TA, Wang JY, Jung JW, Mace D, Pointer S, Barron C, Brady SM, Schiefelbein J, Benfey PN (2008) Cell identity mediates the response of Arabidopsis roots to abiotic stress. Science **320:** 942–945

Dudev T, Nikolova V (2016) Determinants of Fe^{2+} over M^{2+} (M = Mg, Mn, Zn) selectivity in non-heme iron proteins. Inorg Chem **55:** 12644–12650

Edgar RC (2004) MUSCLE: Multiple sequence alignment with high accuracy and high throughput. Nucleic Acids Res **32:** 1792–1797

Gasch P, Fundinger M, Müller JT, Lee T, Bailey-Serres J, Mustroph A (2016) Redundant ERF-VII transcription factors bind an evolutionarily conserved cis-motif to regulate hypoxia-responsive gene expression in Arabidopsis. Plant Cell **28:** 160–180

Gibbs J, Greenway H (2003) Mechanisms of anoxia tolerance in plants. I. Growth, survival and anaerobic catabolism. Funct Plant Biol **30:** 1–47

Gibbs DJ, Lee SC, Isa NM, Gramuglia S, Fukao T, Bassel GW, Correia CS, Corbineau F, Theodoulou FL, Bailey-Serres J, et al (2011) Homeostatic response to hypoxia is regulated by the N-end rule pathway in plants. Nature **479:** 415–418

Gibbs DJ, Isa NM, Movahedi M, Lozano-Juste J, Mendiondo GM, Berckhan S, Marín-de la Rosa N, Vicente Conde J, Sousa Correia C, Pearce SP, et al (2014) Nitric oxide sensing in plants is mediated by proteolytic control of group VII ERF transcription factors. Mol Cell **53:** 369–379

Giuntoli B, Shukla V, Maggiorelli F, Giorgi FM, Lombardi L, Perata P, Licausi F (2017) Age-dependent regulation of ERF-VII transcription factor activity in *Arabidopsis thaliana*. Plant Cell Environ **40:** 2333–2346

Graciet E, Wellmer F (2010) The plant N-end rule pathway: Structure and functions. Trends Plant Sci **15:** 447–453

Irving H, Williams RJP (1948) Order of stability of metal complexes. Nature **162:** 746–747

Isebrands JG, Richardson J (2014) Poplars and Willows: Trees for Society and the Environment. CABI, Boston, MA

Kosmacz M, Parlanti S, Schwarzländer M, Kragler F, Licausi F, Van Dongen JT (2015) The stability and nuclear localization of the transcription factor RAP2.12 are dynamically regulated by oxygen concentration. Plant Cell Environ **38:** 1094–1103

Kreuzwieser J, Furniss S, Rennenberg H (2002) Impact of waterlogging on the N-metabolism of flood tolerant and non-tolerant tree species. Plant Cell Environ **25:** 1039–1049

Kreuzwieser J, Hauberg J, Howell KA, Carroll A, Rennenberg H, Millar AH, Whelan J (2009) Differential response of gray poplar leaves and roots underpins stress adaptation during hypoxia. Plant Physiol **149:** 461–473

Kumar S, Stecher G, Li M, Knyaz C, Tamura K (2018) MEGA X: Molecular evolutionary genetics analysis across computing platforms. Mol Biol Evol **35:** 1547–1549

Lanquar V, Ramos MS, Lelièvre F, Barbier-Brygoo H, Krieger-Liszkay A, Krämer U, Thomine S (2010) Export of vacuolar manganese by AtNRAMP3 and AtNRAMP4 is required for optimal photosynthesis and growth under manganese deficiency. Plant Physiol **152:** 1986–1999

Lanquar V, Grossmann G, Vinkenborg JL, Merkx M, Thomine S, Frommer WB (2014) Dynamic imaging of cytosolic zinc in Arabidopsis roots combining FRET sensors and RootChip technology. New Phytol **202:** 198–208

Licausi F, van Dongen JT, Giuntoli B, Novi G, Santaniello A, Geigenberger P, Perata P (2010) HRE1 and HRE2, two hypoxia-inducible ethylene response factors, affect anaerobic responses in *Arabidopsis thaliana*. Plant J **62:** 302–315

Licausi F, Kosmacz M, Weits DA, Giuntoli B, Giorgi FM, Voesenek LACJ, Perata P, van Dongen JT (2011) Oxygen sensing in plants is mediated by an N-end rule pathway for protein destabilization. Nature **479:** 419–422

Lichtenthaler HK (1987) Chlorophylls and carotenoids: Pigments of photosynthetic membranes. Methods Enzymol **148:** 350–382

Livak KJ, Schmittgen TD (2001) Analysis of relative gene expression data using real-time quantitative PCR and the 2(-Δ Δ C(T)) method. Methods **25:** 402–408

Lloyd G, McCown B (1980) Commercially-feasible micropropagation of mountain laurel, *Kalmia latifolia*, by use of shoot-tip culture. IPPS Combined Proceedings **30:** 421–427

Long XX, Yang XE, Ni WZ, Ye ZQ, He ZL, Calvert DV, Stoffella JP (2003) Assessing zinc thresholds for phytotoxicity and potential dietary toxicity in selected vegetable crops. Commun Soil Sci Plant Anal **34:** 10016

Loreti E, Valeri MC, Novi G, Perata P (2018) Gene regulation and survival under hypoxia requires starch availability and metabolism. Plant Physiol **176:** 1286–1298

Lumba S, Toh S, Handfield LF, Swan M, Liu R, Youn JY, Cutler SR, Subramaniam R, Provart N, Moses A, et al (2014) A mesoscale abscisic acid hormone interactome reveals a dynamic signaling landscape in Arabidopsis. Dev Cell **29:** 360–372

Maret W (2013) Inhibitory zinc sites in enzymes. Biometals **26:** 197–204

Müller A, Volmer K, Mishra-Knyrim M, Polle A (2013) Growing poplars for research with and without mycorrhizas. Front Plant Sci **4:** 332

Murashige T, Skoog F (1962) A revised medium for rapid growth and bio assays with tobacco tissue cultures. Physiol Plant **15:** 473–497

Mustroph A, Zanetti ME, Jang CJH, Holtan HE, Repetti PP, Galbraith DW, Girke T, Bailey-Serres J (2009) Profiling translatomes of discrete cell populations resolves altered cellular priorities during hypoxia in Arabidopsis. Proc Natl Acad Sci USA **106:** 18843–18848

Nakano T, Suzuki K, Fujimura T, Shinshi H (2006) Genome-wide analysis of the ERF gene family in Arabidopsis and rice. Plant Physiol **140:** 411–432

Olsen LI, Palmgren MG (2014) Many rivers to cross: The journey of zinc from soil to seed. Front Plant Sci **5:** 30

Ou B, Yin KQ, Liu SN, Yang Y, Gu T, Wing Hui JM, Zhang L, Miao J, Kondou Y, Matsui M, et al (2011) A high-throughput screening system for Arabidopsis transcription factors and its application to Med25-dependent transcriptional regulation. Mol Plant **4:** 546–555

Pajevi S, Bori M, Arsenov DD, Milan Ž (2016) Phytoextraction of heavy metals by fast-growing trees: A review. *In* AA Ansari, SS Gill, R Gill, GR Lanza, L Newman, eds, Phytoremediation. Springer, Cham, Switzerland, pp 29–65

Pilon-Smits E (2005) Phytoremediation. Annu Rev Plant Biol **56:** 15–39

Ranjan A, Dickopf S, Ullrich KK, Rensing SA, Hoecker U (2014) Functional analysis of COP1 and SPA orthologs from Physcomitrella and rice during photomorphogenesis of transgenic Arabidopsis reveals distinct evolutionary conservation. BMC Plant Biol **14:** 178

Ricachenevsky FK, Menguer PK, Sperotto RA, Fett JP (2015) Got to hide your Zn away: Molecular control of Zn accumulation and biotechnological applications. Plant Sci **236:** 1–17

Romeo S, Francini A, Ariani A, Sebastiani L (2014) Phytoremediation of Zn: Identify the diverging resistance, uptake and biomass production behaviours of poplar clones under high zinc stress. Water Air Soil Pollut **225:** 1–12

Romeo S, Francini A, Sebastiani L, Morabito D (2017) High Zn concentration does not impair biomass, cutting radial growth, and photosynthetic activity traits in *Populus alba* L. J Soils Sediments **17:** 1394–1402

Sasidharan R, Hartman S, Liu Z, Martopawiro S, Sajeev N, van Veen H, Yeung E, Voesenek LACJ (2018) Signal dynamics and interactions during flooding stress. Plant Physiol **176:** 1106–1117

Schuler M, Bauer P (2011) Heavy metals need assistance: The contribution of nicotianamine to metal circulation throughout the plant and the Arabidopsis NAS gene family. Front Plant Sci **2:** 69

Sebastiani L, Francini A, Romeo S, Ariani A, Minnocci A (2014) Heavy metals stress on poplar: Molecular and anatomical modifications. *In* P Sharma and RK Gaur,, eds, Approaches to Plant Stress and Their Management. Springer, New Delhi, India, pp 267–279

Shahzad Z, Canut M, Tournaire-Roux C, Martinière A, Boursiac Y, Loudet O, Maurel C (2016) A potassium-dependent oxygen sensing pathway regulates plant root hydraulics. Cell **167:** 87–98.e14

Sharma SS, Dietz KJ, Mimura T (2016) Vacuolar compartmentalization as indispensable component of heavy metal detoxification in plants. Plant Cell Environ **39:** 1112–1126

Shi WG, Li H, Liu TX, Polle A, Peng CH, Luo ZB (2015) Exogenous abscisic acid alleviates zinc uptake and accumulation in *Populus*×*canescens* exposed to excess zinc. Plant Cell Environ **38:** 207–223

Sinclair SA, Krämer U (2012) The zinc homeostasis network of land plants. Biochim Biophys Acta **1823:** 1553–1567

Sivitz AB, Hermand V, Curie C, Vert G (2012) Arabidopsis bHLH100 and bHLH101 control iron homeostasis via a FIT-independent pathway. PLoS ONE **7:** e44843

Tripathy BC, Pattanayak GK (2012) Chlorophyll biosynthesis in higher plants. *In* JJ Eaton-Rye, BC Tripathy, TD Sharkey, eds, Photosynthesis: Advances in Photosynthesis and Respiration. Springer, Dordrecht, The Netherlands, pp 63–94

Tsednee M, Yang SC, Lee DC, Yeh KC (2014) Root-secreted nicotianamine from *Arabidopsis halleri* facilitates zinc hypertolerance by regulating zinc bioavailability. Plant Physiol **166:** 839–852

van Dongen JT, Licausi F (2015) Oxygen sensing and signaling. Annu Rev Plant Biol **66:** 345–367

Varshavsky A (2019) N-degron and C-degron pathways of protein degradation. Proc Natl Acad Sci USA **116:** 358–366

Vicente J, Mendiondo GM, Movahedi M, Peirats-Llobet M, Juan YT, Shen YY, Dambire C, Smart K, Rodriguez PL, Charng YY, et al (2017) The Cys-Arg/N-end rule pathway is a general sensor of abiotic stress in flowering plants. Curr Biol **27:** 3183–3190.e4

Weits DA, Giuntoli B, Kosmacz M, Parlanti S, Hubberten HM, Riegler H, Hoefgen R, Perata P, van Dongen JT, Licausi F (2014) Plant cysteine oxidases control the oxygen-dependent branch of the N-end-rule pathway. Nat Commun **5:** 3425

Weits DA, Kunkowska AB, Kamps NCW, Portz K, Packbier NK, Nemec-Venza Z, Gaillochet C, Lohmann JU, Pedersen O, van Dongen JT, et al (2019) An apical hypoxic niche sets the pace over shoot meristem activity. Nature10.1038/s41586-019-1203-6

White MD, Klecker M, Hopkinson RJ, Weits DA, Mueller C, Naumann C, O'Neill R, Wickens J, Yang J, Brooks-Bartlett JC, et al (2017) Plant cysteine oxidases are dioxygenases that directly enable arginyl transferase-catalysed arginylation of N-end rule targets. Nat Commun **8:** 14690

White MD, Kamps JJAG, East S, Taylor Kearney LJ, Flashman E (2018) The plant cysteine oxidases from *Arabidopsis thaliana* are kinetically tailored to act as oxygen sensors. J Biol Chem **293:** 11786–11795

Yadav SK (2010) Heavy metals toxicity in plants: An overview on the role of glutathione and phytochelatins in heavy metal stress tolerance of plants. S Afr J Bot **76:** 167–179

Yoo SD, Cho YH, Sheen J (2007) Arabidopsis mesophyll protoplasts: A versatile cell system for transient gene expression analysis. Nat Protoc **2:** 1565–1572

Zhuang J, Cai B, Peng RH, Zhu B, Jin XF, Xue Y, Gao F, Fu XY, Tian YS, Zhao W, et al (2008) Genome-wide analysis of the AP2/ERF gene family in *Populus trichocarpa*. Biochem Biophys Res Commun **371:** 468–474